Linear transient growth of coherent structure in turbulent channel flow at low Reynolds number

Aiko Yakeno

JAMSTEC
Showa-machi 3173-25, Kanazawa-ku,
Yokohama-city, Kanagawa, 236-0001, Japan
yakeno@jamstec.go.jp

Takahiro Tsukahara

Tokyo University of Science
Yamazaki 2641, Noda-shi,
Chiba 278-8510, Japan
tsuka@rs.tus.ac.jp

ABSTRACT

We have conducted the linear transient growth analysis on a turbulent channel flow at very low Reynolds number, such as $Re_\tau = 50$, with considering a nonlinear turbulence effect by eddy viscosity. The maximum growth rate of perturbation at a certain target time was computed and the optimal mode for the case was detected. It is known when the flow is in a subcritical turbulent transitional state of a very low Reynolds number, localized turbulent structures are observed and turbulent spots are transitionally distributed in the streamwise and spanwise directions to form a long stripe pattern over a whole computation domain (Tsukahara & Ishida, 2014). What underlies the transition mechanism and how the pattern is generated have not been clarified well in detail. In the present transient growth analysis, we compared three flow conditions: laminar, turbulent at $Re_\tau = 50$ and 500, in order to obtain specific features for the case of very low Reynolds number. Note that no energy growth was detected if the flow was laminar of that Reynolds number, while, with the turbulence condition, perturbation energy temporally increased to approximately ten times larger at the maximum than that of its initial state. The high Reynolds number case results of $Re_\tau = 500$ for whole target times basically corresponded to those of reference studies (Del Álamo & Jiménez, 2006; Pujals *et al.*, 2009). On the other hand, the low Reynolds number case of the present study, $Re_\tau = 50$, showed different aspects of characteristics. Secondly, we analyzed the maximum growth rate in detail for three limited target times. A wavelength of the dominant mode which had the most kinetic energy in each target case enlarged as the target time became longer among tested ones. It is noted the two-dimensional growth not only in the spanwise direction but also in the streamwise direction ($\lambda_x/d = 2 \sim 3$) was observed at a short target time. Thirdly, vectors and contour lines of wall-normal, spanwise and streamwise perturbation velocities in $z-y$ plane of each wavelength mode and time series of their transient growth were presented. Although we need further investigation on how linear transient amplification affects on generating a long laminar-turbulence stripe pattern observed in DNS, the present facts show dependency of the optimal transient mode on Reynolds number and a target time, those possibly bring a new knowledge for coherent structure specially at transitional low Reynolds numbers.

INTRODUCTION

Nonlinear hydrodynamic stability theory has been concerned for years, with phenomena such as transition to turbulence, which is still challenging theme to understand. Firstly Reynolds (1883) mentioned about importance of nonlinear disturbances of Poiseuille flow in a pipe, Bohr (1909), Heisenberg (1951) and Landau (1944) treated them theoretically. In these years, it has been reported that fundamental features of such turbulent near-wall streak and streamwise roll-structure in channel flow were well predicted by transient growth theory based on a highly non-normal operator of a strong sheared flow (Butler & Farrell, 1992; Trefethen *et al.*, 1993; Reddy & Henningson, 1993; Farrell *et al.*, 2017). Recently, as for turbulent channel flow, Del Álamo & Jiménez (2006) directly simulated the maximum transient growth rate of perturbation based on the linearized Navier-Stokes equations with turbulence mean velocity and turbulence eddy viscosity. It was found that streamwise elongated structures generally experience large transient growth and the transient growth rate had two prominent peaks at distinct spanwise wavelengths, which Pujals *et al.* (2009) confirmed later too. One of them is scaled by wall viscous units as $\lambda_z^+ \approx 100$ and corresponds to that of near-wall streak. The variable with a superscript of $+$ represents normalization by viscous scale units. The other one is scaled with outer units such as a channel half width, d, as $\lambda_z/d \approx 4$, which is independent on the Reynolds number. This fact agrees well with the dominance of very large scale motion (VLSM) or large scale motion (LSM) observed in experiment (Kim & Adrian, 1999) and direct numerical simulation (DNS) (Abe *et al.*, 2001; Del Álamo & Jiménez, 2003), which implies that transient growth processes play a significant role in the coherent motion, although their spanwise wavelength are reported as $\lambda_z/d = 1.5 \sim 2$.

As for the low Reynolds numbers, DNS by Tsukahara & Ishida (2014) showed that the localized turbulence in a form of oblique band was distributed in the streamwise and spanwise directions to form a long stripe pattern. At low friction Reynolds numbers below $Re_\tau = 80$, the stripe pattern exhibits an obliquity angle of about 25 degree against the streamwise direction. As the Reynolds number decreases and approaches the lower limit of the transitional regime, the obliquity angle becomes 45 degree. The formation mechanism of the stripe pattern, the selection of obliquity angle have been unclear. In such a low Reynolds number flow, the spanwise wavelength of a near-wall streak structure, $\lambda_z^+ \approx 100$, reaches to a channel width, $2d$. Nonlinear interaction of the inner and the outer scale motions seems to occur, which is not negligible. The present study gives a new sight of transient growth of linear amplification in such a low Reynolds number flow as the first step.

PROCEDURE

Computational condition

The evolution equations for the disturbance generally is derived by considering a basic state $(\bar{u}_i^+, \bar{p}^+)$, and a perturbed state (u'^+_i, p'^+), both satisfying the Navier-Stokes equations. Perturbation equations with turbulence eddy viscosity for the transient growth analysis are expressed as follows,

$$\frac{\partial u'^+_i}{\partial t^+} + \frac{\partial}{\partial x_j^+}\left(\bar{u}_i^+ u'^+_j + u'^+_i \bar{u}_j^+\right) = -\frac{\partial p'^+}{\partial x_i^+} + \frac{\partial}{\partial x_j^+}\left(\nu_T^+ \frac{\partial u'^+_i}{\partial x_j^+}\right). \tag{1}$$

We assume that the flow is homogeneous in the streamwise, x, and spanwise directions ,z. We apply the total eddy viscosity normalized

in viscous wall units, which is described as $\nu_T^+ = \nu_T/\nu = 1+\nu_t^+$, to consider the turbulence effect of nonlinear terms in the equations. In the present case, the turbulent mean velocity profile, $\bar{u}^+$, is defined as follows,

$$\frac{\partial \bar{u}^+}{\partial(\eta)} = -\frac{Re_\tau \eta}{\nu_T^+}, \tag{2}$$

where $\eta = y/d$ and $Re_\tau = u_\tau d/\nu$. We use turbulent eddy viscosity, ν_t^+, suggested by Reynolds & Tiederman (1967) as same as Del Álamo & Jiménez (2006) and Pujals *et al.* (2009) did for the case of the higher Reynolds number channel flow.

$$\begin{aligned} f_1 &= 1-\eta^2, \quad f_2 = 1+2\eta^2, \\ f_3 &= 1-\exp\left(-\frac{(1-|\eta|)Re_\tau}{A}\right), \\ \nu_t^+ &= 0.5\left\{1+\left(\frac{\kappa Re_\tau f_1 f_2 f_3}{3}\right)^2\right\}^{1/2} - 0.5 \end{aligned} \tag{3}$$

Turbulence mean velocity, $\bar{u}^+$, and total eddy viscosity, ν_T^+, are shown for the cases of $Re_\tau = 50$ and 500 in Fig. 1a and Fig. 1b, respectively. Parameters A and κ are set as $A = 26.5$ and $\kappa = 0.426$. Values of $\bar{u}^+$ are calculated with ν_T^+ on the basis of Eq. (2). In the present study, $\bar{v}^+$ and $\bar{w}^+$ are set as zero. For a comparison, we perform the case of Poiseuille laminar flow with keeping the same bulk mean velocity as that of turbulent flow of $Re_\tau = 50$. DNS results at $Re_\tau = 50$ show that turbulence bands are distributed and forming a long stripe pattern in the whole computational domain among subcritical turbulence atmosphere. The turbulence eddy viscosity used in the study is much smaller than that in the case of $Re_\tau = 500$. It does not model the nonlinear turbulence motion of the transitional flow state perfectly. For the future analyses, that nonlinear effect will be considered.

Computational method

We compute the maximum transient growth rate by using the strategy that Barkley *et al.* (2008) reported. Perturbation equations, Eq. (1), are described with the linear evolution operator, $\mathbf{A}(t)$, and a variable matrix, $\mathbf{u}'$.

$$\mathbf{u}'(t) = \mathbf{A}(t)\mathbf{u}_0'. \tag{4}$$

The perturbation growth rate at a certain target time, τ, is described as the inner vector as follows.

$$\frac{E(\tau)}{E(0)} = (\mathbf{A}(\tau)\mathbf{u}_0', \mathbf{A}(\tau)\mathbf{u}_0') = (\mathbf{u}_0', \mathbf{A}(\tau)^*\mathbf{A}(\tau)\mathbf{u}_0'). \tag{5}$$

The initial mode, $\mathbf{v}_j$, is computed as the eigenfunction of the self-adjoint operator, $\mathbf{A}(\tau)^*\mathbf{A}(\tau)$. This gives the eigenvalue, λ_j, as the growth rate.

$$\mathbf{A}(\tau)^*\mathbf{A}(\tau)\cdot\mathbf{v}_j = \lambda_j \mathbf{v}_j, \qquad \| \mathbf{v}_j \| = 1 \tag{6}$$

On the basis of this concept, the maximum transient growth rate, $G_{max}(\tau)$, is computed as the maximum eigenvalue, λ_j, of the self-adjoint operator of $\mathbf{A}(\tau)$, with the optimal mode matrix.

$$G_{max}(\tau) = \max_{\|\mathbf{u}'(0)\|=1} \frac{E(\tau)}{E(0)} = \max_j \lambda_j. \tag{7}$$

In the present study for the turbulent channel flow, since the base flow $\overline{u_i}$ in Eq. (1) is considered to be homogeneous in the streamwise and spanwise directions, all perturbation are expressed in Fourier space.

$$u_i'(x,y,z,t) = \hat{u}_i(y,t)\exp\left(i(K_x x + K_z z)\right), \tag{8}$$

$$p'(x,y,z,t) = \hat{p}(y,t)\exp\left(i(K_x x + K_z z)\right). \tag{9}$$

The variable with a hat superscript means a Fourier coefficient, while K_x and K_z denote the streamwise and spanwise wave numbers. The streamwise and spanwise wave lengths are given by $\lambda_x = 2\pi/K_x$ and $\lambda_z = 2\pi/K_z$, respectively. For each combination of (K_x, K_z), the maximum transient growth rate, G_{max}, at a certain target time, τ, is computed. In the study, computation grid number in the wall-normal direction, y, is 129 for whole cases. Time step is $\Delta t u_\tau/d = 0.005$.

Verification study of the presently developed code was conducted. This is based on comparison of G_{max} with those obtained by Butler & Farrell (1992) for the case of laminar Poiseuille flow, and those by Pujals *et al.* (2009) for turbulent channel flow at the same Reynolds number condition.

RESULTS AND DISCUSSION

Maximum transient growth

We conduct transient growth computations for three cases: Poiseuille laminar flow, turbulence flow at $Re_\tau = 50$ and 500. At first, we compute the optimal growth rate for whole target times, from $\tau u_\tau/d = 0.05$ to 5.0, and obtain an envelope value for each wavelength mode, G_{global}. This is described as follows;

$$G_{global} = \max_\tau G_{max}(\tau). \tag{10}$$

It is noted that no energy growth was detected if the flow was laminar of that Reynolds number, while, with the turbulence condition, perturbation energy temporally increased to approximately ten times larger at the maximum than that of the initial state. These values are shown in Fig.2a for $Re_\tau = 50$ and Fig.2b for $Re_\tau = 500$, respectively. Results of high Reynolds number case of $Re_\tau = 500$ basically corresponds to those of reference studies (Del Álamo & Jiménez, 2006; Pujals *et al.*, 2009). We identify two prominent peaks at the spanwise wavelength of $\lambda_z/d = 0.2$ (100 in viscous wall units) and $\lambda_z/d = 4$, with condition that roughly $\lambda_x > \lambda_z$. The present low Reynolds number study of $Re_\tau = 50$ showed different aspects of characteristics. The peak of $\lambda_z^+ = 100$ in viscous wall units is not apparent approximately at $\lambda_z/d = 2$ in Fig.2a, although that at $\lambda_z/d = 4$ is prominent. It is interesting there is a small peak of $\lambda_x/d = 2 \sim 3$, which is true only in the low Reynolds number case.

At second, we analyze the maximum growth rate for three limited target times, $\tau u_\tau/d = 0.1$, 0.6 and 1.0, for the case of turbulent channel flow at low Reynolds number. A wavelength of the dominant mode in each target case enlarges linearly as the target time became longer among tested ones in the present study, though that is not shown in this paper. Maximum transient growth rates of Eq. (7) for each target time are shown in Fig.3a, Fig.3b and Fig.3c. We observe that the dominant wavelength mode and its amplitude depends on the target time. It is noted two-dimensional growth in the streamwise direction ($\lambda_x/d = 2 \sim 3$) appears at a short target time as

shown in Fig.3a. That target time corresponds to $t^+(=tu_\tau^2/\nu)=5.0$ in viscous wall units. This fact is drawing an attention, which mode is one of the potential factors to cause a stripe pattern of turbulence in a channel, although the amplification rate is not large and the time period is short.

Optimal growth modes

We focus on the optimal growth mode for each target time, which has the most kinetic energy growth, with assuming a two-dimensional growth as K_x equals to zero; (1) $\lambda_z/d = 1.0$ for $\tau u_\tau/d = 0.1$, (2) $\lambda_z/d = 2.0$ for $\tau u_\tau/d = 0.6$, (3) $\lambda_z/d = 3.0$ for $\tau u_\tau/d = 1.0$. For a reference, the dominant mode of $\lambda_z/d = 4.0$ needs a target time of $\tau u_\tau/d = 2.0$. We detect vectors and contour lines of wall-normal, spanwise and streamwise perturbation velocities in $z-y$ plane of each wavelength mode as shown in Figs.4. These values are calculated on the basis of Eq. (8). In Figs.4, left lined figures show the initial states ($t=0$), right lined ones do the maximally growing states ($t=\tau$). Contour color lines represent perturbation in the streamwise direction, u'. Blue tiny arrays are perturbation vectors in the wall-normal and the spanwise direction, (v',w'). Black dotted-lines are drawn to clarify the flow direction in figures. The streamwise roll-vortices appear in each figure, with different scales and shapes. At a short target time, small vortices are generated only near the wall. As the target time is longer, largest vortices scale becomes larger.

Time series of their kinetic energy growth, $E(t)/E(0)$, are shown in Fig.5. The optimal mode for a short target time ($\tau u_\tau/d = 0.1$) grows and shrinks faster than other modes. It is left for the future analysis whether the small scale mode dynamics affects on the larger scale one. Though we need further investigation what this transient growth plays a role in subcritical Reynolds number flow to generate a long turbulence stripe pattern observed in DNS, the present facts refer dependency of the optimal transient growth mode on the turbulence condition, Reynolds number and a target time, those possibly bring a new knowledge for turbulent channel flow specially at transitional low Reynolds numbers.

CONCLUSION

We have conducted the transient growth analysis on turbulent channel flow at very low Reynolds number, $Re_\tau = 50$. We have computed the maximum transient growth rate for three target times, and found some specific characteristics for turbulence channel flow at very low Reynolds number. This fact has a possibility to become one of the milestones to explain the stripe pattern formation of laminar-turbulence coexistence, at the low Reynolds number of subcritical transitional state. We need further investigation on effects of modes interaction in a transitional state. and will consider a sophisticated nonlinear model and compare results with DNS ones.

ACKNOWLEDGEMENT

A. Y. acknowledges the support of the Grant-in-Aid for Scientific Research (B) (No. 15K21677). T. T. acknowledges the supports of the Grant-in-Aid for Scientific Research (A) (No. 16H06066) and on Innovative Areas (No. 16H00813) by Ministry of Education, Culture, Sports, Science and Technology of Japan.

REFERENCES

Abe, H., Kawamura, H. & Matsuo, Y. 2001 Direct Numerical Simulation of a Fully Developed Turbulent Channel Flow With Respect to the Reynolds Number Dependence. *Journal of Fluids Engineering* **123** (2), 382.

Barkley, D., Blackburn, H. M. & Sherwin, S. J. 2008 Direct optimal growth analysis for timesteppers. *International Journal for Numerical Methods in Fluids* **57**, 1435–1458.

Bohr, N. 1909 Determination of the surface-tension of water by the method of jet vibration. *Philosophical Transactions of the Royal Society of London. Series A, Containing Papers of a Mathematical or Physical Character* **209**, 281–317.

Butler, K. M. & Farrell, B. F. 1992 Three-dimensional optimal perturbations in viscous shear flow. *Physics of Fluids* **4** (8), 1637–1650.

Del Álamo, J. C. & Jiménez, J. 2003 Spectra of the very large anisotropic scales in turbulent channels. *Physics of Fluids* **15** (6), L41.

Del Álamo, J. C. & Jiménez, J. 2006 Linear energy amplification in turbulent channels. *Journal of Fluid Mechanics* **559**, 205.

Farrell, B. F., Ioannou, P. J. & Nikolaidis, M.-A. 2017 Instability of the roll-streak structure induced by background turbulence in pretransitional Couette flow. *Physical Review Fluids* **2**, 1–16.

Heisenberg, W. 1951 On stability and turbulence of fluid flows .

Kim, K. C. & Adrian, R. J. 1999 Very large-scale motion in the outer layer. *Physics of Fluids* **11** (2), 417–422.

Landau, L. D 1944 On the problem of turbulence. In *Dokl. Akad. Nauk SSSR*, , vol. 44, pp. 339–349.

Pujals, G., Garcia-Villalba, M., Cossu, C. & Depardon, S. 2009 A note on optimal transient growth in turbulent channel flows. *Physics of Fluids* **21**, 015109.

Reddy, S. C. & Henningson, D. S. 1993 Energy growth in viscous channel flows. *Journal of Fluid Mechanics* **6**, 209–238.

Reynolds, O. 1883 An experimental investigation of the circumstances which determine whether the motion of water shall be direct or sinuous, and of the law of resistance in parallel channels. *Proceedings of the royal society of London* **35** (224-226), 84–99.

Reynolds, W. C. & Tiederman, W. G. 1967 Stability of turbulent channel flow, with application to malkus's theory. *Journal of Fluid Mechanics* **27** (02), 253–272.

Trefethen, L. N., Trefethen, A. E., Reddy, S. C. & Driscoll, T. A. 1993 Hydrodynamic Stability Without Eigenvalues. *Science* **261**, 578–584.

Tsukahara, T. & Ishida, T. 2014 The lower bound of subcritical transition in plane poiseuille flow. In *EUROMECH, Colloquium EC565*.

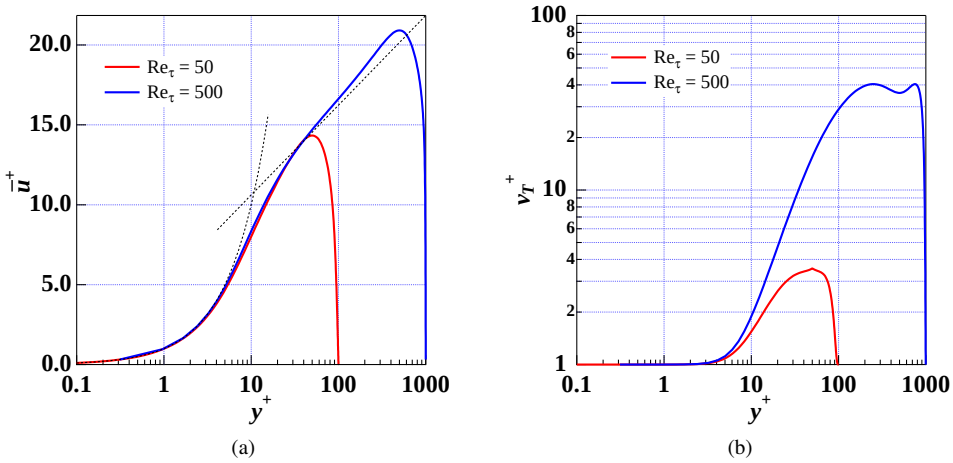

Figure 1: Base flow conditions based on Eqs.(3), when $A = 26.5$ and $\kappa = 0.41$; (a) mean streamwise velocity, $\bar{u}^+$ and (b) total eddy viscosity, ν_T^+ for turbulent cases of $Re_\tau = 50$ and 500.

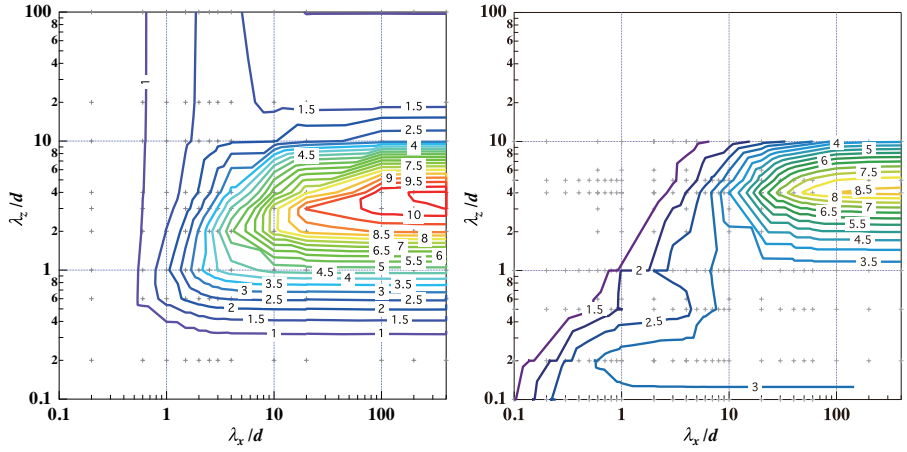

Figure 2: Envelope value of the maximum growth rate for whole target times, G_{global} ; (a) $Re_\tau = 50$ and (b) 500.

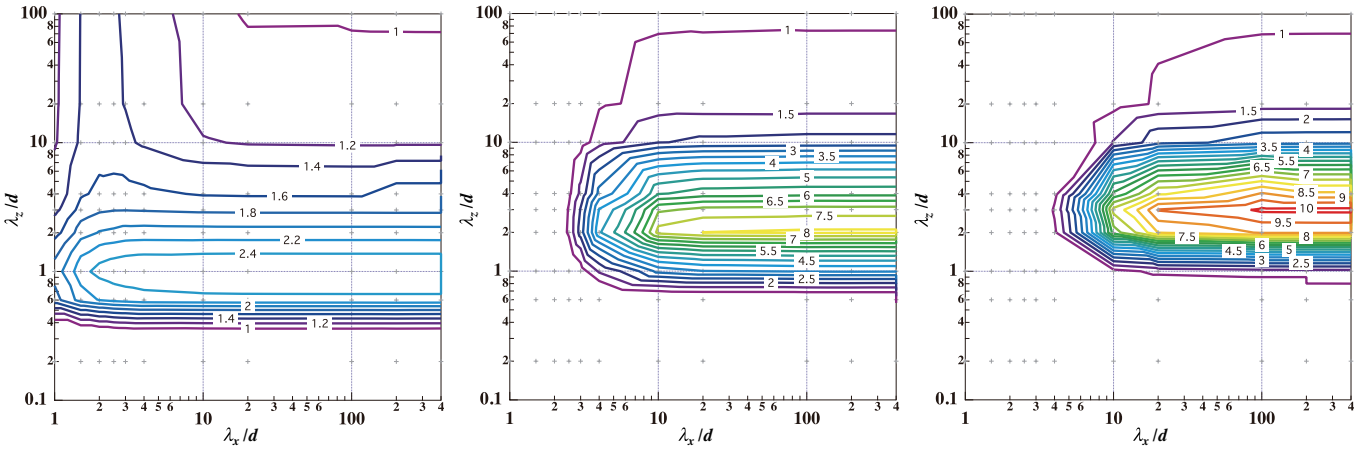

Figure 3: Maximum growth rate at target times, G_{max} (τ), at $Re_\tau = 50$; (a) $\tau u_\tau/d = 0.1$, (b) 0.6 and (c) 1.0.

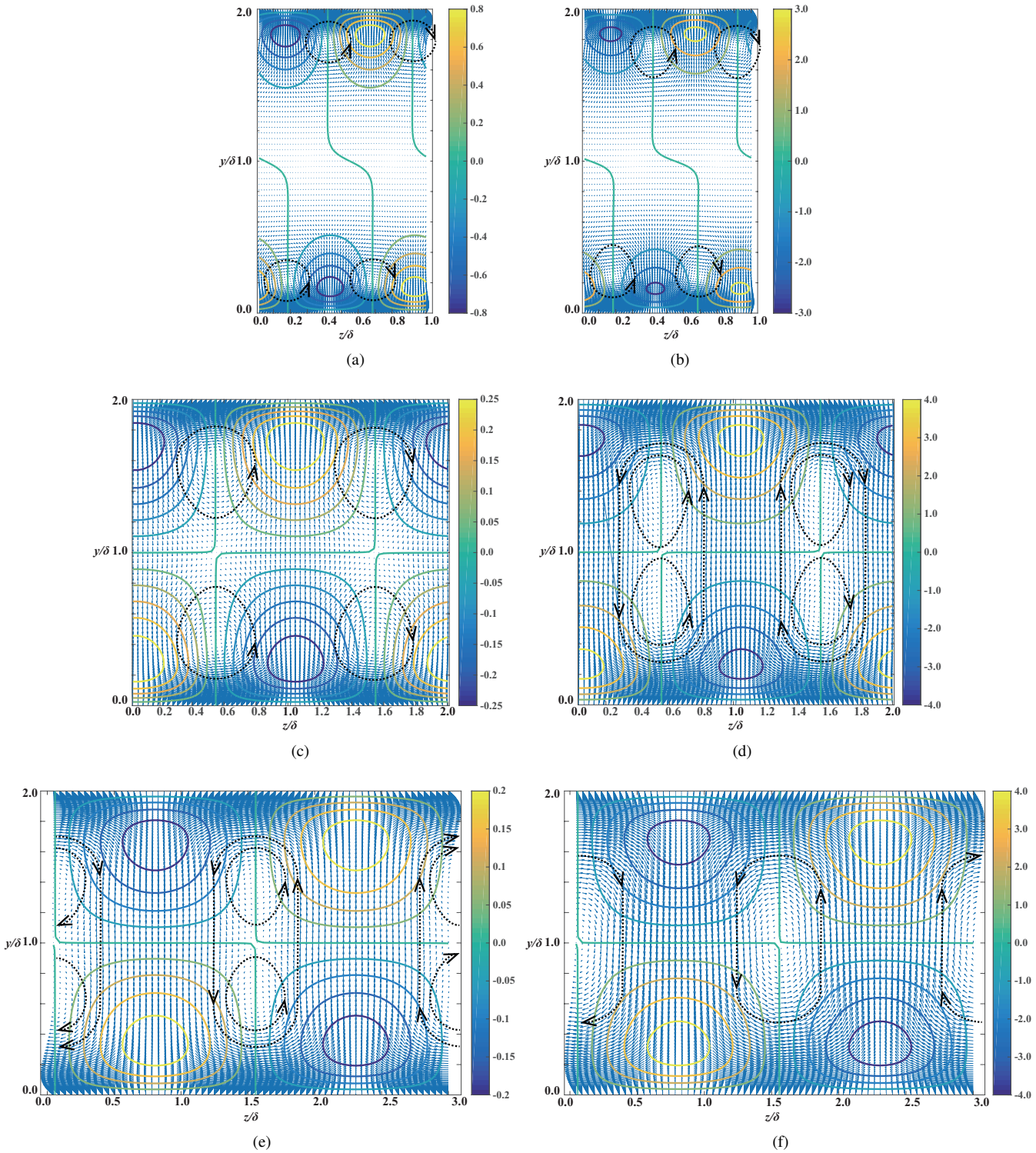

Figure 4: Optimal growth mode with $K_x = 0$ for target times; (a) (b) $\tau u_\tau/d = 0.1$, (c) (d) 0.6 and (e) (f) 1.0, initial state (left line) and the maximally growing states (right line), at $Re_\tau = 50$. Contour color lines represent u', blue vectors are (v', w') and black dotted-lines with arrays are drawn for flow direction.

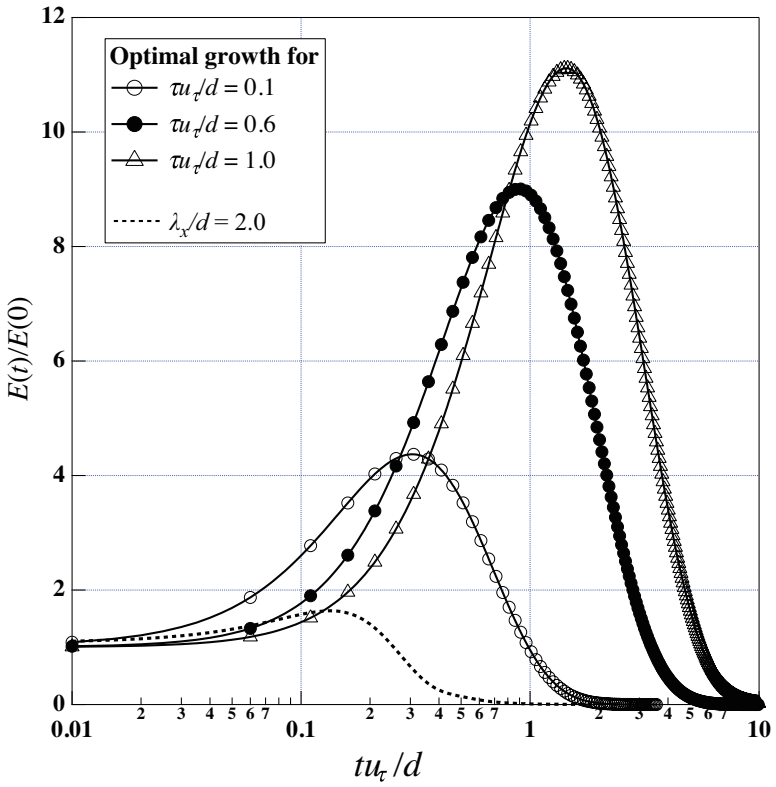

Figure 5: Time series of kinetic energy growth, $E(t)/E(0)$, of optimal modes with $K_x = 0$ for three target times at $Re_\tau = 50$. Dotted line represents the case of $(\lambda_x/d, \lambda_z/d) = (2.0,\infty)$.